Competitive Adsorption of Molybdenum in the Presence of Phosphorus or Sulfur on Gibbsite

Sabine Goldberg

Abstract: Anion adsorption on the aluminum oxide, gibbsite, was investigated as a function of solution pH (3–11) and equilibrium solution Mo (3.13, 31.3, or 313 μmol/L), P (96.9 μmol/L), or S (156 μmol/L) concentration. Adsorption of all three anions decreased with increasing pH. Electrophoretic mobility measurements indicated a downward shift in point of zero charge, indicative of an inner-sphere adsorption mechanism for all three anions. The constant capacitance model, having an inner-sphere adsorption mechanism, was able to describe Mo and P adsorption; whereas the triple-layer model with an outer-sphere adsorption mechanism was used to describe S adsorption. Competitive adsorption experiments showed a reduction of Mo adsorption at a Mo/P ratio of 1:30 and 1:300 but no reduction at a Mo/S ratio of 1:52 and 1:520. These concentrations are realistic of natural systems where Mo is found in much lesser concentrations than P or S. Using surface complexation constants from single-ion systems, the triple-layer model predicted that even elevated S concentrations did not affect Mo adsorption. The constant capacitance model was able to predict the competitive effect of P on Mo adsorption semiquantitatively.

Key words: Constant capacitance model, triple-layer model, surface complexation model.

(*Soil Sci* 2010;175: 105–110)

Molybdenum is an essential trace element for both plants and animals. For plant growth, Mo is the essential micronutrient required in the smallest amount. The minimum Mo requirement for animal nutrition is also very low. Levels of Mo in soils are usually extremely small, 0.5 to 5 mg L^{-1} (Gupta and Lipsett, 1981). Although Mo rarely causes harmful effects or yield reductions in crops under field conditions, it is readily taken up, especially by legumes, and can accumulate to levels that are toxic to grazing ruminant animals (Reisenauer et al., 1973). Excessive soil solution Mo concentrations can occur, primarily on alkaline soils in the western United States, especially in the San Joaquin Valley of California (Barshad, 1948). Detailed knowledge of the geochemical factors that influence Mo availability is necessary both to optimize plant Mo nutrition and for management of soils high in Mo.

Aluminum oxide content is one of the soil factors that affects availability of Mo to plants (Reisenauer et al., 1973). Molybdenum adsorption by soils was found to be highly correlated with extractable Al (Barrow, 1970). Although Mo sorption has been investigated on a wide range of crystalline Al oxides, most of these studies dealt with high-temperature alumina, Al_2O_3 (Ferreiro et al., 1985; Spanos et al., 1990a, 1990b; Vordonis et al., 1990; Spanos and Lycourghiotis, 1994; El Shafei et al., 2000; Vissenberg et al., 2000). The studies of Goldberg et al. (1996, 1998) and Manning and Goldberg (1996) on gibbsite and Ferreiro et al. (1985) on bayerite are the only investigations of Mo adsorption by crystalline Al oxide minerals found in soils. Gibbsite is the most common crystalline Al oxide mineral present in soils. The pitfalls of using thermodynamically unstable high-temperature Al oxides to study adsorption were demonstrated by Goldberg and Glaubig (1988) who showed that the location of the B adsorption maximum shifted downward by 1.5 pH units in just 24 h of reaction time because of dissolution.

Description of Mo adsorption behavior on gibbsite requires knowledge of the mode of binding of the Mo anions on the mineral surface. Insight into ion adsorption mechanisms can be provided by macroscopic experimental observations such as point of zero charge (PZC) shifts and ionic strength effects on extent of ion adsorption. Molybdenum adsorption reduced the PZC of gibbsite, indicating strong specific adsorption and inner-sphere surface complexation (Goldberg et al., 1996). Molybdenum adsorption on gibbsite showed little ionic strength dependence, also indirect evidence of inner-sphere surface complex formation (Goldberg et al., 1998).

Molybdenum adsorption reactions by Al oxides and soils have generally been studied in single-anion systems, or at most, in the presence of one competing anion species. Molybdenum adsorption studies were carried out on soils (Roy et al., 1986) in the presence of equimolar phosphate concentration and on γ-Al_2O_3 in the presence of equimolar sulfate concentration (Wu et al., 2001). Although the presence of phosphate depressed Mo adsorption on soils, Mo adsorption on alumina was unaffected by the presence of equimolar sulfate.

Recognizing that phosphate and sulfate occur at higher concentrations than Mo in nature, studies on soils have been conducted at Mo/P molar ratios of 1:5 (Brinton and O'Connor, 2000), 1:9 (Xie and MacKenzie, 1991), and 1:10 (Gonzalez et al., 1974) and at Mo/S molar ratios of 1:5 (Brinton and O'Connor, 2000), 1:6 (Smith et al., 1987), and 1:10 (Gonzalez et al., 1974). Reductions in Mo adsorption were observed in all of the phosphate studies and some of the sulfate studies (Brinton and O'Connor, 2000; Smith et al., 1987). Only in the study of Gorlach et al. (1969) were Mo, S, and P added in proportions realistic for soils. At a 1:140 molar ratio of Mo/P, reductions in Mo adsorption were observed; whereas at a 1:240 molar ratio of Mo/S, no effect of S on Mo adsorption was noted. The lack of competitive effect of the presence of sulfate in the study of Gorlach et al. (1969) was not caused by differences in Fe or Al oxide content or organic matter content because their soils were intermediate in these properties between those of Smith et al. (1987) and Xie and MacKenzie (1991).

Molybdenum adsorption on gibbsite has been described using two surface complexation modeling approaches: constant capacitance model (Manning and Goldberg, 1996; Goldberg et al., 1996, 1998) and triple-layer model (Goldberg et al., 1998). The constant capacitance model was able to describe Mo adsorption on gibbsite (Manning and Goldberg, 1996). The triple-layer

USDA-ARS, U.S. Salinity Laboratory, 450 W. Big Springs Rd, Riverside, CA 92507. Dr. Sabine Goldberg is corresponding author. E-mail: sabine.goldberg@ars.usda.gov
Received September 29, 2009.
Accepted for publication January 7, 2010.

ISSN: 0038-075X
DOI: 10.1097/SS.0b013e3181d3462f

model was able to describe simultaneous Mo and sulfate adsorption on γ-Al_2O_3 (Wu et al., 2001) and Mo adsorption on amorphous Al oxide (Goldberg et al., 2008).

The objectives of this study were to (i) investigate Mo adsorption on gibbsite at Mo concentrations realistic to natural systems, (ii) investigate the effect of competing sulfate and phosphate ions on Mo adsorption by gibbsite at concentrations of S and P realistic for soil systems, and (iii) evaluate the ability of the chemical surface complexation models to describe Mo adsorption in both the single-ion and the competitive systems.

MATERIALS AND METHODS

Molybdenum adsorption was investigated on a hydrated alumina S-11 obtained from the Aluminum Company of America (Alcoa Center, PA). Using an X-ray diffraction powder mount, the material was found to consist of gibbsite without any detectable impurities. Specific surface area was determined to be 18.0 $m^2\ g^{-1}$ from a single-point BET N_2 adsorption isotherm obtained using a Quantasorb Jr surface area analyzer (Quantachrome Corp, Syosset, NY).

Points of zero charge for the gibbsite were determined by microelectrophoresis using a Zeta-Meter 3.0 system (Zeta Meter, Long Island City, NY). The electrophoretic mobilities of suspensions containing 0.01% gibbsite in 0.015 *M* NaCl were determined at various pH values. Points of zero charge were obtained by linear interpolation of the data to zero electrophoretic mobility. Electrophoretic mobility measurements were also determined in the presence of 31.3, 52.1, 73.0, 104 μmol/L Mo, 9.69, 96.9, 969 μmol/L P, 156 μmol/L or 1.56 mmol/L S.

Adsorption experiments were carried out in batch systems to determine anion adsorption envelopes (amount of anion adsorbed as a function of solution pH per fixed total anion concentration). Samples of 0.2 g of gibbsite were added to 250-mL polypropylene centrifuge bottles and equilibrated with 100 mL of a 0.1 *M* NaCl solution by shaking for 20 h on a reciprocating shaker at 23 °C ± 0.3 °C. The equilibrating solutions contained 3.13, 31.3, or 313 μmol/L Mo, or 96.9 μmol/L P, or 156 μmol/L S and had been adjusted to the desired pH values using 1.0 *M* HCl or 1.0 *M* NaOH that changed the total volume by 2% or less. The samples were centrifuged, and the decantates were analyzed for pH, filtered through 0.45-μm membrane filters, and analyzed for Mo, P, or S concentrations using inductively coupled plasma optical emission spectrometry.

Competitive adsorption experiments were carried out with equilibrating solutions containing 3.13 μmol/L Mo and P concentrations of 9.69, 96.9, or 969 μmol/L, or S concentrations of 156 μmol/L or 1.56 mmol/L. The anions were added simultaneously. The experimental procedure remained the same as for the single-anion adsorption experiments previously described.

The constant capacitance model (Stumm et al., 1980) was used to describe molybdate and phosphate adsorption behavior. The description of sulfate adsorption behavior was improved by use of the triple-layer model (Davis et al., 1978). Acid-base reactions for molybdic acid: $pK_a^1 = 4.00$, $pK_a^2 = 4.24$; and phosphoric acid: $pK_a^1 = 2.22$, $pK_a^2 = 9.20$, $pK_a^3 = 20.7$ were included (Lindsay, 1979). In both models, the protonation and dissociation reactions are:

$$AlOH_{(s)} + H^+_{(aq)} \leftrightarrow AlOH^+_{2\,(s)} \quad (1)$$

$$AlOH_{(s)} \leftrightarrow AlO^-_{(s)} + H^+_{(aq)} \quad (2)$$

where $AlOH_{(s)}$ represents a reactive surface hydroxyl in the gibbsite mineral. The surface complexation reactions for molybdate and phosphate adsorption are defined to form inner-sphere surface complexes:

$$AlOH_{(s)} + H_2MoO_{4(aq)} \leftrightarrow AlHMoO_{4(s)} + H_2O \quad (3)$$

$$AlOH_{(s)} + H_3PO_{4(aq)} \leftrightarrow AlH_2PO_{4(s)} + H_2O \quad (4)$$

$$AlOH_{(s)} + H_3PO_{4(aq)} \leftrightarrow AlHPO^-_{4\,(s)} + H^+_{(aq)} + H_2O \quad (5)$$

$$AlOH_{(s)} + H_3PO_{4(aq)} \leftrightarrow AlPO^{2-}_{4\,(s)} + 2H^+_{(aq)} + H_2O \quad (6)$$

whereas the surface complexation reaction for sulfate adsorption is defined to form an outer-sphere surface complex:

$$AlOH_{(s)} + SO^{2-}_{4\,(aq)} + H^+_{(aq)} \leftrightarrow AlOH^+_2 - SO^{2-}_{4\,(s)} \quad (7)$$

The triple-layer model includes outer-sphere surface complex formation for the background electrolyte:

$$AlOH_{(s)} + Na^+_{(aq)} \leftrightarrow AlO^- - Na^+_{(s)} + H^+_{(aq)} \quad (8)$$

$$AlOH_{(s)} + H^+_{(aq)} + Cl^-_{(aq)} \leftrightarrow AlOH^+_2 - Cl^-_{(s)} \quad (9)$$

Equilibrium constants for the surface complexation reactions are defined as:

$$K_+(\text{int}) = \frac{[AlOH^+_2]}{[AlOH][H^+]} \exp(F\psi_o/RT) \quad (10)$$

$$K_-(\text{int}) = \frac{[AlO^-][H^+]}{[AlOH]} \exp(-F\psi_o/RT) \quad (11)$$

$$K_{Na^+}(\text{int}) = \frac{[AlO^- - Na^+][H^+]}{[AlOH][Na^+]} \exp[F(\psi_\beta - \psi_o)/RT] \quad (12)$$

$$K_{Cl^-}(\text{int}) = \frac{[AlOH^+_2 - Cl^-]}{[AlOH][H^+][Cl^-]} \exp[F(\psi_o - \psi_\beta)/RT] \quad (13)$$

$$K_{Mo}(\text{int}) = \frac{[AlHMoO_4]}{[AlOH][H_2MoO_4]} \quad (14)$$

$$K^1_P(\text{int}) = \frac{[AlH_2PO_4]}{[AlOH][H_3PO_4]} \quad (15)$$

$$K^2_P(\text{int}) = \frac{[AlHPO^-_4][\text{H}^+]}{[AlOH][H_3PO_4]} \exp(-F\psi_o/RT) \quad (16)$$

$$K^3_P(\text{int}) = \frac{[AlPO^{2-}_4][\text{H}^+]^2}{[AlOH][H_3PO_4]} \exp(-2F\psi_o/RT) \quad (17)$$

$$K_s(\text{int}) = \frac{[AlOH^+_2 - SO^{2-}_4]}{[AlOH][SO^{2-}_4][\text{H}^+]} \exp[F(\psi_o - 2\psi_\beta)/RT] \quad (18)$$

where F is the Faraday constant (C mol_c^{-1}), Ψ is the surface potential (V), R is the molar gas constant (J mol^{-1} K^{-1}), T is the absolute temperature (K), square brackets indicate concentrations (mol L^{-1}), o refers to the surface plane of inner-sphere adsorption, and β refers to the plane of outer-sphere adsorption. The exponential terms can be considered as solid-phase activity coefficients (Sposito, 1983).

The computer program FITEQL 3.2 (Herbelin and Westall, 1996) was used to fit the anion surface complexation constants to the experimental adsorption data in single-anion systems. The FITEQL code uses a nonlinear least squares optimization routine to fit equilibrium constants to experimental data and contains both the constant capacitance and the triple-layer models of

adsorption. For the competitive systems, the models were used to predict anion adsorption using the equilibrium constants previously determined for the single-anion systems without optimizing any additional adjustable parameters.

The surface site density was treated as anion-reactive site density and was set to the maximum anion adsorption obtained in the experiments. Constant capacitance model values for the protonation constant, log K_+(int) = 7.38, and the dissociation constant, log K_-(int) = −9.09, were obtained from a literature compilation of experimental values for Al oxides (Goldberg and Sposito, 1984). Triple-layer model surface complexation constant values for the protonation constant, log K_+(int) = 5.0, the dissociation constant, log K_-(int) = −11.2, and the background electrolyte surface complexation constants, log K_{Na+} = −8.6 and log K_{Cl-} = 7.5, were obtained from the study of Sprycha (1989a, 1989b) on γ-Al_2O_3.

The constant capacitance model capacitance value was fixed at C = 1.06 F m^{-2}, considered optimum for γ-Al_2O_3 (Westall and Hohl, 1980). The triple-layer model capacitance values were fixed at C_1 = 1.2 F m^{-2} and C_2 = F m^{-2}, considered optimum for goethite (Zhang and Sparks, 1990) and used in a prior model application to Mo adsorption by amorphous Al oxide (Goldberg et al., 2008). Goodness of fit was evaluated using the overall variance, V, in Y:

$$V_Y = \frac{SOS}{DF} \tag{19}$$

where SOS is the sum of squares of the residuals and DF is the degrees of freedom.

RESULTS AND DISCUSSION

The PZC of gibbsite in the presence of a background electrolyte of 0.015 *M* NaCl was found to occur at pH 9.1. This PZC value is slightly less than the previous determinations of 9.6 (Goldberg et al., 1996) and 9.8 (Manning and Goldberg, 1996) for gibbsite. The small difference in PZC value is likely caused by the difference in synthesis. The gibbsite of Manning and Goldberg (1996) was prepared by heating to 40 °C and dialyzing, whereas the gibbsite used in the present study, hydrated alumina S-11, was manufactured through a proprietary precipitation process. Figures 1, 2, and 3 present electrophoretic mobility versus pH obtained for gibbsite upon adsorption of Mo, P, and S, respectively. The PZC values are shifted to increasingly lower pH values with increasing anion concentration. These observed changes in PZC value are macroscopic evidence of inner-sphere surface complexation of molybdate, phosphate, and sulfate on gibbsite (Hunter, 1981). The greatest shift in PZC was observed for phosphate adsorption, consistent with the strong adsorption found for this ion on oxide minerals.

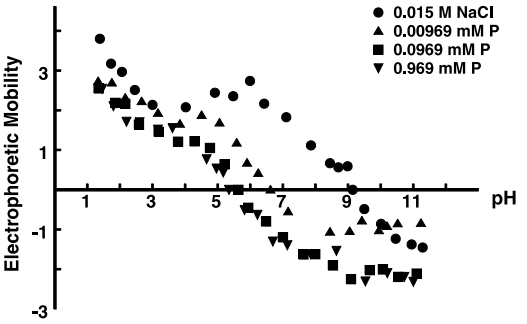

FIG. 2. Electrophoretic mobility of gibbsite as a function of pH and total P concentration in 0.015 *M* NaCl solution. The circles represent zero P treatment.

Anion adsorption on gibbsite as a function of pH is indicated in Figs. 4, 5, and 6 for molybdate, phosphate, and sulfate, respectively. All three ions exhibited decreasing adsorption with increasing solution pH. The adsorption of S and Mo was minimal above pH 7; whereas the adsorption of P decreased more gradually with increasing pH and did not reach minimal levels until above pH 10. The adsorption envelopes of both Mo and P exhibited adsorption maxima around pH 4; whereas the adsorption envelope of S decreased steadily with increasing solution pH.

The ability of the surface complexation models to describe anion adsorption is indicated in Figs. 4, 5, and 6 for Mo, P, and S, respectively. The constant capacitance model was simultaneously optimized for three different Mo concentrations differing by two orders of magnitude. The model fit provided a quantitative description of Mo adsorption at all three Mo concentrations by optimizing only one parameter, the Mo surface complexation constant, log K_{Mo}(int) (Eq.[14]) (Fig. 4). The PZC obtained from the model optimization for 31.3 μmol/L Mo was 8.1, agreeing very well with the experimental PZC of 8.2 (Fig. 1). The constant capacitance model clearly constitutes an advancement over Langmuir and Freundlich adsorption isotherm approaches, which not only contain two empirical adjustable parameters, but also cannot describe changes in adsorption occurring with changes in solution pH.

The constant capacitance model was fit to P adsorption using three P surface complexation constants (Eqs.[15], [16], and [17]). The fit was only semiquantitative in that the model

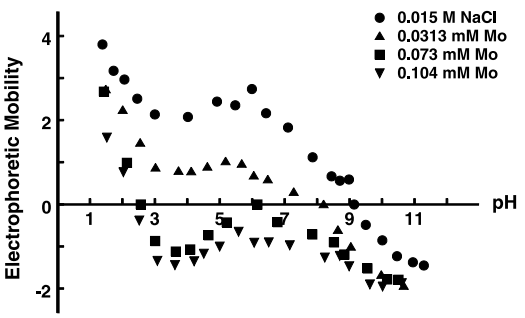

FIG. 1. Electrophoretic mobility of gibbsite as a function of pH and total Mo concentration in 0.015 *M* NaCl solution. The circles represent zero Mo treatment.

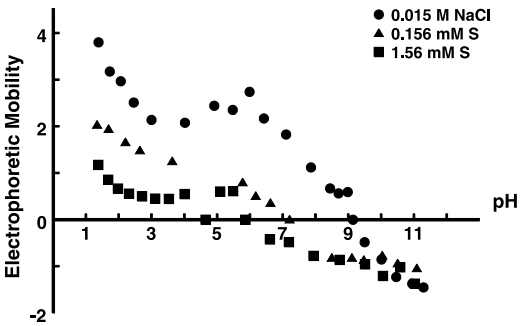

FIG. 3. Electrophoretic mobility of gibbsite as a function of pH and total S concentration in 0.015 *M* NaCl solution. The circles represent zero S treatment.

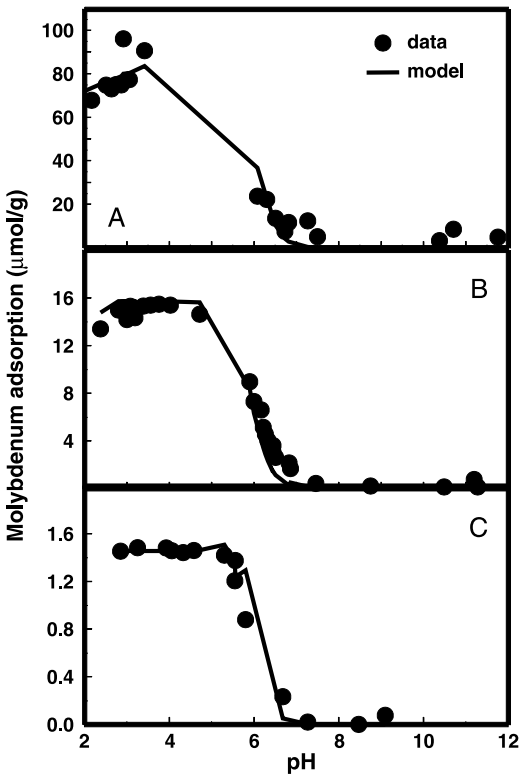

FIG. 4. Molybdenum adsorption as a function of solution Mo concentration and pH: (A) 3.13 μmol/L; (B) 31.3 μmol/L; (C) 313 μmol/L. Experimental data are represented by solid circles. Constant capacitance model fits are represented by solid lines. Log K_{Mo}(int) = 7.54, V_Y = 30.4.

failed to describe the phosphate adsorption maximum occurring at pH 4 (Fig. 5). Overall, the fit of the model to the data was closest in the pH range 5.5 to 8.5. Fortunately, most agricultural soils fall into this pH range. Bleam et al. (1991) maintained solubility equilibrium through addition of $AlCl_3$ in their study of phosphate adsorption on the Al oxide, boehmite. They obtained

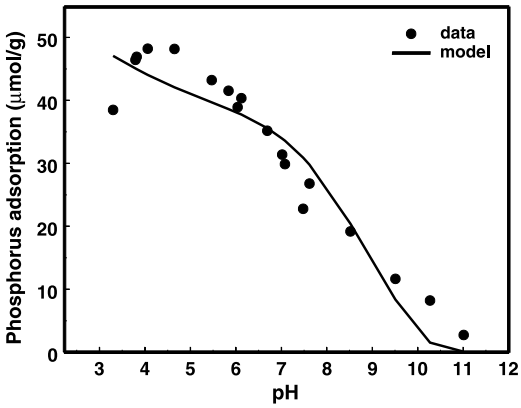

FIG. 5. Phosphorus adsorption as a function of solution pH from an equilibrating solution of P = 96.9 μmol/L. Experimental data are represented by solid circles. The constant capacitance model fit is represented by a solid line. Log K^1_P(int) = 7.81, Log K^2_P(int) = 2.86, Log K^3_P(int) = −3.48, V_Y = 36.4.

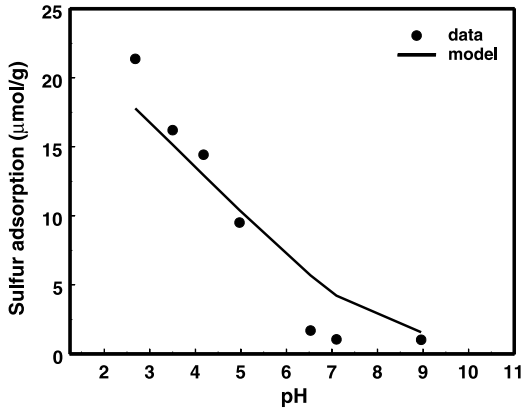

FIG. 6. Sulfur adsorption as a function of solution pH from an equilibrating solution of S = 156 μmol/L. Experimental data are represented by solid circles. The triple layer model fit is represented by a solid line. Log K_S(int) = 11.49, V_Y = 22.3.

a constant capacitance model description of the phosphate adsorption maximum at pH 4 only after various Al-PO_4 solution species were included. Such a model description might also have been possible in our study if Al concentrations had been available. The PZC obtained from the model optimization for 96.9 μmol/L P was 6.4, in reasonable agreement with the experimental PZC of 5.8 (Fig. 2).

The constant capacitance model and the triple-layer model were each fit to S adsorption using one surface complexation constant. The fit of the triple-layer model using an outer-sphere S surface complex, Eq.(7), was much improved over that of the constant capacitance model having an inner-sphere S surface complex, as evidenced by a 3-fold decrease in variance, the goodness-of-fit criterion: V_Y(CCM) = 66.2 versus V_Y(TLM) = 22.3 (Fig. 6). This result would suggest that an outer-sphere adsorption mechanism is more appropriate for describing sulfate adsorption on gibbsite. Prior analyses of sulfate adsorption on γ-Al_2O_3 using Raman and Fourier Transform Infrared spectroscopies had indicated the formation of predominantly outer-sphere surface complexes with a small fraction of inner-sphere surface complexes (Wijnja and Schulthess, 2000). This could also be the case for sulfate adsorption in our study. The shifts in PZC upon sulfate adsorption (Fig. 3) were smaller than those observed upon molybdate (Fig. 1) and phosphate adsorption (Fig. 2). This could happen if only a small fraction of the sulfate surface complexes are inner-sphere. Outer-sphere surface complex formation would not change the PZC (Hunter, 1981). The PZC obtained from the model optimization for 156 μmol/L S was 8.0, in reasonable agreement with the experimental PZC of 7.2 (Fig. 3). The PZC value from the model optimization must be considered approximate because it was obtained by linear interpolation over a very large pH range, 7 to 9.

The ability of the surface complexation models to predict anion adsorption from competitive systems using the surface complexation constants obtained for single-ion systems was evaluated. The constant capacitance model was used to predict molybdate and phosphate adsorption from mixed systems of both anions. The Mo concentration remained constant at 3.13 μmol/L, whereas the phosphate concentrations were 3×, 30×, and 300× the Mo concentration. As can be seen in Fig. 7A, the extent of Mo adsorption was unaffected by the presence of 3× equimolar phosphate concentration over the entire pH range. Further increases in the P concentration to

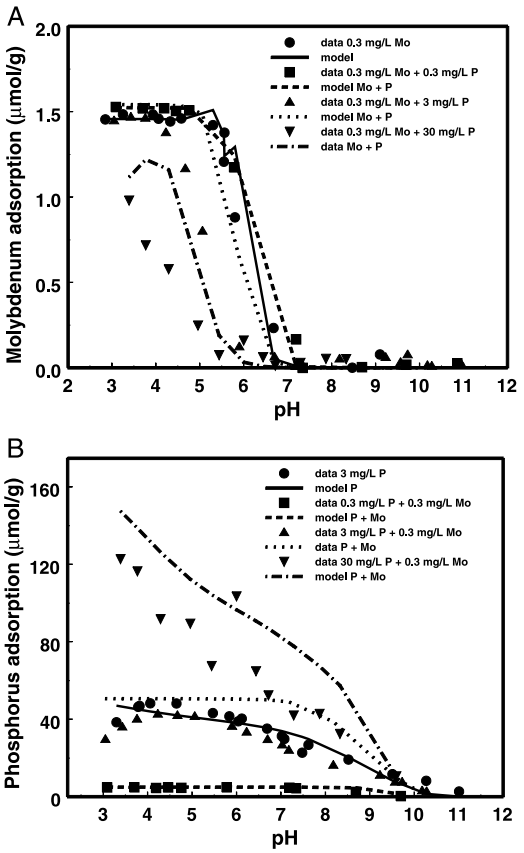

FIG. 7. Competitive adsorption as a function of solution P concentration and pH: (A) Mo adsorption; (B) P adsorption. Experimental data are represented by solid symbols. Constant capacitance model predictions are represented by lines.

30× and 300× progressively decreased Mo adsorption. The presence of Mo at one third equimolar did not affect phosphate adsorption (Fig. 7B). This result is not surprising given the low concentration of Mo and is in agreement with the findings of Roy et al. (1986) that the adsorption of phosphate on soils was not greatly suppressed by the presence of Mo. The constant capacitance model predicted a decrease in Mo adsorption in the presence of phosphate that was less than that experimentally observed (Fig. 7A). The model was able to predict phosphate adsorption at various solution phosphate concentrations in the presence of Mo (Fig. 7B).

The triple-layer model was used to predict molybdate and sulfate adsorption from mixed systems of both anions. In the triple-layer model application, the surface complexes were defined as inner-sphere for Mo adsorption and outer-sphere for S adsorption as had been determined in the single-ion systems. Again, the Mo concentration remained constant at 3.13 μmol/L, whereas the sulfate concentrations were 52× and 520× the Mo concentration. As can be seen in Fig. 8A, the extent of Mo adsorption was unaffected by the presence of both of these sulfate concentrations. This result is in agreement with the findings of Gorlach et al. (1969) that the adsorption of molybdate on soils was not affected by the presence of S at a Mo/S ratio of 1:240. The presence of Mo at 3.13 μmol/L did not affect sulfate adsorption at 156 μmol/L (Fig. 8B). This result is not surprising given the extremely low concentrations of Mo in relation to sulfate. Consistent with the experimental observations, the triple-layer model predicted no effect of the presence of large concentrations of sulfate on Mo adsorption (Fig. 8A). This result is expected given that the model application defines sulfate as a weak outer-sphere surface complex and molybdate as a strong inner-sphere surface complex. The model was able to quantitatively describe sulfate adsorption at the 156 μmol/L concentration but considerably underpredicted sulfate adsorption at the higher 1.56 mmol/L concentration (Fig. 8B).

Molybdate adsorption was investigated at 3.13 μmol/L, a small concentration realistic for natural systems. Competitive adsorption studies in the presence of phosphate at 300× and sulfate at 520× the concentration of Mo, representative of natural systems, were carried out. The Mo adsorption was unaffected by the presence of S concentrations up to 520×, whereas Mo adsorption was depressed in the presence of P at 30× and 300×. The constant capacitance model was well able to describe Mo and P adsorption in single-ion systems but underpredicted the competitive effect in mixed systems. The triple-layer model was able to describe Mo and S adsorption in single-ion systems and in mixed systems where no competitive effect was found. Our study suggests that Mo adsorption would be unaffected by the presence of S but decreased by the presence of P at field-realistic concentrations. This finding is significant for the incorporation of these adsorption reactions into chemical speciation-transport models for use in predicting anion behavior in soils.

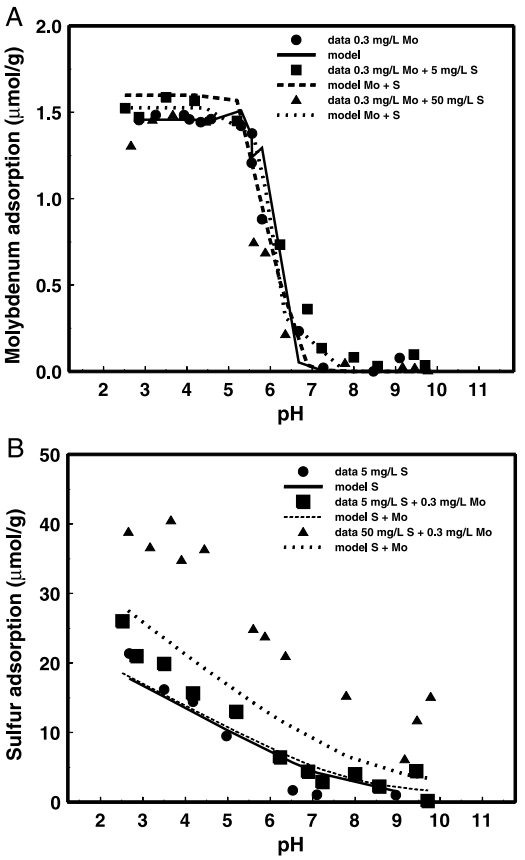

FIG. 8. Competitive adsorption as a function of solution S concentration and pH: (A) Mo adsorption; (B) S adsorption. Experimental data are represented by solid symbols. Triple layer model predictions are represented by lines.

ACKNOWLEDGMENTS

The author thanks Ms V. Sann, Ms P. Xiong, Ms J. Zuwayed, and Mr H.S. Forster for technical assistance.

REFERENCES

Barrow, N. J. 1970. Comparison of the adsorption of molybdate, sulfate and phosphate by soils. Soil Sci. 109:282–288.

Barshad, I. 1948. Molybdenum content of pasture plants in relation to toxicity to cattle. Soil Sci. 66:187–195.

Bleam, W. F., P. E. Pfeffer, S. Goldberg, R. W. Taylor, and R. Dudley. 1991. A 31P solid-state nuclear magnetic resonance study of phosphate adsorption at the boehmite/aqueous solution interface. Langmuir 7:1702–1712.

Brinton, S. R., and G. A. O'Connor. 2000. Factors affecting molybdenum sorption in soils: Potential biosolids effects. Soil Crop Sci. Soc. Florida Proc. 59:117–123.

El Shafei, G. M. S., N. A. Moussa, and C. A. Philip. 2000. Association of molybdenum ionic species with alumina surface. J. Colloid Interface Sci. 228:105–113.

Ferreiro, E. A., A. K. Helmy, and S. G. de Bussetti. 1985. Molybdate sorption by oxides of aluminium and iron. Z. Planzenernaehr. Bodenk. 148:559–566.

Davis, J. A., R. O. James, and J. O. Leckie. 1978. Surface ionization and complexation at the oxide/water interface: I. Computation of electrical double layer properties in simple electrolytes. J. Colloid Interface Sci. 63:480–499.

Goldberg, S., and R. A. Glaubig. 1988. Boron and silicon adsorption on an aluminum oxide. Soil Sci. Soc. Am. J. 52:87–91.

Goldberg, S., and G. Sposito. 1984. A chemical model of phosphate adsorption by soils. I. Reference oxide minerals. Soil Sci. Soc. Am. J. 48:772–778.

Goldberg, S., H. S. Forster, and C. L. Godfrey. 1996. Molybdenum adsorption on oxides, clay minerals, and soils. Soil Sci. Soc. Am. J. 60:425–432.

Goldberg, S., C. T. Johnston, D. L. Suarez, and S. M. Lesch. 2008. Mechanism of molybdenum adsorption on soils and soil minerals evaluated using vibrational spectroscopy and surface complexation modeling. *In:* Adsorption of Metals by Geomedia II: Variables, Mechanisms, and Model Applications. Developments in Earth & Environmental Sciences 7. M. O. Barnett and D. B. Kent (eds.). Elsevier, Amsterdam, the Netherlands, pp. 235–266.

Goldberg, S., C. Su, and H. S. Forster. 1998. Sorption of molybdenum on oxides, clay minerals, and soils: Mechanisms and models. *In:* Adsorption of Metals by Geomedia: Variables, Mechanisms, and Model Applications, Proc. Am. Chem. Soc. Symp. E. A. Jenne (ed.). Academic Press, San Diego, CA, pp. 401–426.

Gonzalez, B. R., H. Appelt, E. B. Schalscha, and F. T. Bingham. 1974. Molybdate adsorption characteristics of volcanic-ash–derived soils in Chile. Soil Sci. Soc. Am. Proc. 38:903–906.

Gorlach, E., K. Gorlach, and A. Compala. 1969. The effect of phosphate on the sorption and desorption of molybdates from soil. Agrochimica 13:506–512.

Gupta, U. C., and J. Lipsett. 1981. Molybdenum in soils, plants, and animals. Advan. Agron. 34:73–115.

Herbelin, A. L., and J. C. Westall. 1996. FITEQL: A computer program for determination of chemical equilibrium constants from experimental data. Rep. 96-01, Version 3.2, Dept. of Chemistry, Oregon State Univ., Corvallis.

Hunter, R. J. 1981. Zeta Potential in Colloid Science. Principles and Applications. Academic Press, London, UK.

Lindsay, W. L. 1979. Chemical Equilibria in Soils. John Wiley & Sons, New York, NY.

Manning, B. A., and S. Goldberg. 1996. Modeling competitive adsorption of arsenate with phosphate and molybdate on oxide minerals. Soil Sci. Soc. Am. J. 60:121–131.

Reisenauer, H. M., L. M. Walsh, and R. G. Hoeft. 1973. Testing soils for sulphur, boron, molybdenum, and chlorine. *In:* Soil Testing and Plant Analysis, rev. ed. L. M. Walsh and J. D. Beaton (eds.). SSSA, Madison, WI, pp. 173–200.

Roy, W. R., J. J. Hassett, and R. A. Griffin. 1986. Competitive coefficients for the adsorption of arsenate, molybdate, and phosphate mixtures by soils. Soil Sci. Soc. Am. J. 50:1176–1182.

Smith, C., K. W. Brown, and L. E. Deul. 1987. Plant availability and uptake of molybdenum as influenced by soil type and competing ions. J. Environ. Qual. 16:377–382.

Spanos, N., and A. Lycourghiotis. 1994. Molybdenum-oxo species deposited on alumina by adsorption. III. Advances in the mechanism of $Mo^{(VI)}$ deposition. J. Catal. 147:57–71.

Spanos, N., L. Vordonis, Ch. Kordulis, and A. Lycourghiotis. 1990a. Molybdenum-oxo species deposited on alumina by adsorption. I. Mechanism of the adsorption. J. Catal. 124:301–314.

Spanos, N., L. Vordonis, Ch. Kordulis, P. G. Koutsoukos, and A. Lycourghiotis. 1990b. Molybdenum-oxo species deposited on alumina by adsorption. II. Regulation of the surface Mo^{VI} concentration by control of the protonated surface hydroxyls. J. Catal. 124:315–323.

Sposito, G. 1983. On the surface complexation model of the oxide-aqueous solution interface. J. Colloid Interface Sci. 91:329–340.

Sprycha, R. 1989a. Electrical double layer at alumina/electrolyte interface. I. Surface charge and zeta potential. J. Colloid Interface Sci. 127:1–11.

Sprycha, R. 1989b. Electrical double layer at alumina/electrolyte interface. II. Adsorption of supporting electrolytes. J. Colloid Interface Sci. 127: 12–25.

Stumm, W., R. Kummert, and L. Sigg. 1980. A ligand exchange model for the adsorption of inorganic and organic ligands at hydrous oxide interfaces. Croat. Chem. Acta 53:291–312.

Vissenberg, M. J., L. J. M. Joosten, M. M. E. H. Heffels, A. J. van Welsenes, V. H. J. de Beer, R. A. van Santen, and J. A. R. van Veen. 2000. Tungstate versus molybdate adsorption on oxidic surfaces: A chemical approach. J. Phys. Chem. B 104:8456–8461.

Vordonis, L., P. G. Koutsoukos, and A. Lycourghiotis. 1990. Adsorption of molybdates on doped γ-aluminas in alkaline solutions. Colloids Surf. 50:353–361.

Westall, J., and H. Hohl. 1980. A comparison of electrostatic models for the oxide/solution interface. Adv. Colloid Interface Sci. 12:265–294.

Wijnja, H., and C. P. Schulthess. 2000. Vibrational spectroscopy study of selenate and sulfate adsorption mechanisms on Fe and Al (hydr)oxide surfaces. J. Colloid Interface Sci. 229:286–297.

Wu, C. -H., S. -L. Lo, C. -F. Lin, and C. -Y. Kuo. 2001. Modeling competitive adsorption of molybdate, sulfate, and selenate on γ-Al_2O_3 by the triple-layer model. J. Colloid Interface Sci. 233:259–264.

Xie, R. J., and A. F. MacKenzie. 1991. Molybdate sorption-desorption in soils treated with phosphate. Geoderma 48:321–333.

Zhang, P., and D. L. Sparks. 1990. Kinetics of selenate and selenite adsorption/desorption at the goethite/water interface. Environ. Sci. Technol. 24:1848–1856.

